# Molecular Dynamics Simulation Studies of $CO_2$ – [bmim][$PF_6$] Solutions: Effect of $CO_2$ Concentration

**B. L. Bhargava, A. C. Krishna, and S. Balasubramanian**
Chemistry and Physics of Materials Unit, Jawaharlal Nehru Centre for Advanced Scientific Research, Jakkur, Bangalore 560064, India

*DOI 10.1002/aic.11596*
*Published online August 27, 2008 in Wiley InterScience (www.interscience.wiley.com).*

*Molecular dynamics simulations have been carried out on $CO_2$ – [bmim][$PF_6$] mixtures using a refined atomistic potential model for the ionic liquid, at different concentrations of $CO_2$. The expansion in volume as a function of added $CO_2$ was found to agree well with experiments at all but the highest concentration. Significant concentration dependent differences in the radial distribution function of $CO_2$ around the anion have been observed. These differences have been attributed to the specific interaction between $CO_2$ and the anions. The diffusion coefficients of the ions and of $CO_2$ have been found to increase with increase in $CO_2$ concentration. The rotational relaxation of $CO_2$ molecule in solution is found to be biexponential, and the mean relaxation times decreases with increasing $CO_2$ concentration.* © 2008 American Institute of Chemical Engineers *AIChE J,* 54: 2971–2978, 2008

*Keywords: ionic liquids, supercritical carbon dioxide, molecular dynamics simulation, structure, dynamics*

## Introduction

Room temperature ionic liquids (RTILs), along with supercritical carbon dioxide ($scCO_2$), have been receiving considerable attention from the industry and academia recently.[1] $scCO_2$ is one of the well-studied systems through experimental[2,3] and computational[4–7] approaches. One of the interesting characteristics of $scCO_2$ is its liquid-like density and gas-like transport properties. RTILs, on the other hand, are polar and hence solvate a large number of organic and inorganic compounds. Some of the ILs also possess negligible vapor pressure at ambient conditions[8,9] and a wide liquid range. With a large variety of cations and anions which can be used, in principle, an ionic liquid can be tailor made for a specific application.[10,11] Possessing such interesting properties, these compounds have received a lot of attention in the recent past.[12–22] Supplementary to the experiments, a variety of computational studies have provided microscopic details of these systems.[23–32]

$scCO_2$ has been used for extraction of products from RTILs.[33–36] The interaction between the solute and the solvent in the mixture can impart new properties which the individual components may not possess.[37] Although $CO_2$ is remarkably soluble in imidazolium based ionic liquids,[33,38–43] ionic liquids such as [bmim][$PF_6$] do not dissolve much in $CO_2$.[33,38] The separation of organic compounds and water from ILs using $CO_2$ has been demonstrated.[35] There have been many efforts in the understanding of molecular level interactions between RTIL and $CO_2$.[44–52]

By observing the effects of varying the anion among different ILs, Maginn and coworkers[46] have shown that the anion influences the solubility of $CO_2$ in ionic liquids to a greater extent compared with cation. Earlier, the nature of these anion–$CO_2$ interaction has been probed using vibrational spectroscopic methods.[44] Kazarian et al. have reported a weak Lewis acid–base interaction between $CO_2$ and the

Correspondence concerning this article should be addressed to S. Balasubramanian at bala@jncasr.ac.in.

**Table 1. Details of Simulations**

| $CO_2$ (mol %) | Pressure (MPa) | Box Length (Å) | Density (kg $m^{-3}$) |
|---|---|---|---|
| 0 | 0.0 | 44.30 | 1389 |
| 10 | 0.6 | 44.56 | 1388 |
| 30 | 2.0 | 45.38 | 1378 |
| 50 | 4.4 | 46.81 | 1360 |
| 70 | 15.0 | 49.92 | 1320 |

The uncertainty in the density is less than 0.1%.

anions of the Ils.[44] Computer simulation studies have demonstrated that $CO_2$ occupies preexisting void spaces in the IL that reorganize to accommodate the $CO_2$,[48] which rationalizes for the negligible increase in the molar volume of the mixture compared with pure ILs at low concentration of $CO_2$. X-ray diffraction experiments have been carried out by Kanakubo et al.[49] to examine the intermolecular structure of the solution and, in particular, the location and orientation of the $CO_2$ molecule with reference to the anion. Based on the analysis of experimental data, they have concluded that the $CO_2$ molecule may not be tangential to the $PF_6$ sphere as claimed in the computer simulation studies.[46,48,53]

We have recently carried out ab initio MD simulations of the [bmim][$PF_6$] – $CO_2$ mixture at a $CO_2$ concentration of 70 mol % to study the intermolecular environment around $CO_2$ molecules in the solution.[53] In addition, these ab initio simulations enabled us to refine the interatomic potential model for [bmim][$PF_6$].[54] In the present study, we attempt to study the [bmim][$PF_6$] – $CO_2$ mixture at different concentrations of $CO_2$ using the refined potential model. We present the methods in the next section, followed by the results and end with conclusions drawn from our study.

## Methodology and Simulation Details

Molecular dynamics simulations were carried out on [bmim][$PF_6$] – $CO_2$ mixtures with varying concentration of $CO_2$ at 300 K using the PINY_MD code.[55] The form of the interatomic potential and the potential parameters for the [bmim] and [$PF_6$] ions are adopted from our previous work.[54] The model has been found to predict the intermolecular structure in good agreement with the results of ab initio MD simulations.[53] It also predicts the diffusion coefficients of ions, density, and surface tension in excellent agreement with experimental data. For the $CO_2$ molecules, the EPM2 model[56] was used. Lorentz–Berthelot mixing rules were employed to obtain the Lennard-Jones parameters for cross-interactions. The model contains fully flexible [bmim] and [$PF_6$] ions. However, the bond distances in $CO_2$ were constrained in accordance with the EPM2 model.

Five different systems with 0, 10, 30, 50, and 70 mol % of $CO_2$ in 256 ion pairs of [bmim][$PF_6$] were simulated. The systems were first equilibrated under constant temperature and pressure (NPT) conditions, and later in the canonical (NVT) ensemble, with the volume determined as an average over the earlier NPT trajectory. The number of $CO_2$ molecules for the 10, 30, 50, and 70 mol % of $CO_2$ in solution turned out to be 28, 110, 256, and 595, respectively. The pressure of the system was chosen from experimental data.[57] In the canonical ensemble, the system was equilibrated for at least 2 ns and a trajectory was generated for 2 ns in which the coordinates were stored every 0.9 ps for further analysis. The pressure applied in the isothermal–isobaric ensemble simulation, the converged box length for that pressure and the final densities are provided in Table 1. Other details are as provided earlier.[54]

Nosé-Hoover chain thermostats[58] were used for temperature control with a thermostat time constant of 1 ps. The mean squared displacements of $CO_2$ molecules were found not to be sensitive to the use of thermostats during the analysis phase of the trajectory. Periodic boundary conditions consistent with cubic symmetry were employed to obtain the bulk behavior. Ewald summation method was used to handle Coulombic interactions with an $\alpha$ value of 0.339 $Å^{-1}$. Nonbonded interactions were calculated up to a distance cutoff of 13 Å and long range corrections were applied for the calculation of energy and pressure tensor. The multiple time step algorithm, r-RESPA[59] was used to integrate the equations of motion, in which the nonbonded interactions beyond 6 Å and within 13 Å were integrated with a time step of 3 fs and those within 6 Å with a time step of 1.5 fs. Torsional forces were computed every 0.75 fs and the bending and stretching degrees of freedom were integrated with a time step of 0.375 fs. The energy conservation was monitored through the simulations and was found to be three parts in $10^5$ over 1 ns.

## Results and Discussions

### *Volume expansion*

$CO_2$ is highly soluble in some of the ionic liquids. It is soluble up to 75 mol % in [bmim][$PF_6$].[33] Earlier studies[48] have indicated that $CO_2$ occupies preexisting void spaces in the ionic liquids, which is the reason for the low volume expansion on its addition to the RTILs. Voronoi analysis was used to conclude that the cation and the anion rearrange in the ionic liquid to form small number of large voids from large number of small voids to accommodate the added $CO_2$. It is thus important to verify if the current simulations predict the volume of the solution as a function of $CO_2$ concentration. The volume expansion predicted by the current model at different concentrations of $CO_2$ along with the experimental values[57] are provided in Table 2. The latter are the best fit values obtained by fitting the experimental data to a quadratic equation.

The experimental data were available only in the range of $CO_2$ concentrations between 0 and 56.7 mol %. The values obtained from our simulation are quite close to the experimental data within this domain. The volume expansion for

**Table 2. Comparison of Volume Expansion of [bmim][$PF_6$] – $CO_2$ Mixture at Different Concentrations of $CO_2$ Obtained from Simulations and Experiment[57]**

| Concentration of $CO_2$ (mol %) | Volume Expansion (%) Computation | Volume Expansion (%) Experiment |
|---|---|---|
| 10 | 1.8 | 1.5 |
| 30 | 7.5 | 6.9 |
| 50 | 18.0 | 16.8 |
| 70 | 43.1 | 31.2 |

The uncertainty in the computed value is less than 0.1%.

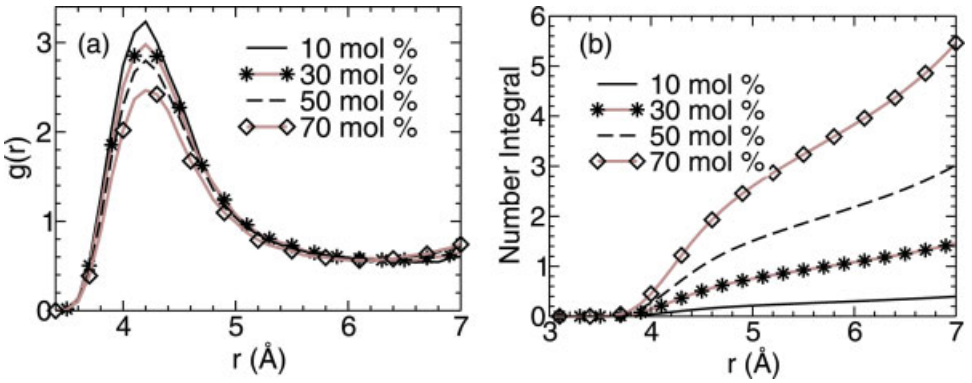


**Figure 1. (a) Radial distribution functions of $CO_2$ around the $PF_6$ anion for different concentrations of $CO_2$ in the solution. Symbols are shown infrequently for clarity; (b) corresponding number integrals.**

[Color figure can be viewed in the online issue, which is available at www.interscience.wiley.com.]

the 70 mol % mixture is quite high in the simulations than the best fit to the experimental data. One of the reasons for this difference may be due to errors in the extrapolation procedure adopted for obtaining the experimental data.

### *Radial distribution functions*

*$PF_6$ – $CO_2$ RDF.* The anion–$CO_2$ radial distribution functions (RDF) and the corresponding running number integrals are presented in Figure 1. The RDF peaks at 4.2 Å at all the concentrations studied. This peak position matches exactly with that reported by Huang et al.[48] The first minimum is present at 6.4 Å for the 50 and 70 mol % mixtures, whereas it is present at 6.2 Å for the 10 and 30 mol % mixtures. Figure 1 clearly shows that there is no shift in the peak positions with the change in the $CO_2$ concentration, although the peak heights are different. The coordination numbers up to 6.3 Å (up to the location of first minimum) are 0.3, 1.2, 2.4, and 4.2, respectively, for the 10, 30, 50, and 70 mol % mixtures. The increase in the coordination number with increase in the $CO_2$ concentration is reasonable. The coordination number up to the first minimum suggests that the $CO_2$ molecules interact with at least two of the anions. This is evident as the number of $CO_2$ that are within the first coordination shell is almost thrice that of the average number of $CO_2$ per anion available in the system. The coordination shell of an anion is not exclusive, that is, the first coordination shell of one anion can overlap with that of the other. In the case of 10, 30, 50, and 70 mol % mixtures, the coordination numbers are found to be 3, 3, 2.5, and 2 times greater than the average number of $CO_2$ per anion, respectively. These suggest that the number of $CO_2$ that can be present in the first coordination shell around the anion is limited by $CO_2$–$CO_2$ repulsion. It has been demonstrated in our previous studies that $CO_2$ occupies the octahedral voids around the anions.[53] Although there are eight such voids, the number of $CO_2$ present around the anion is less than eight, suggesting that steric repulsion between the carbon dioxide molecules or the cation–anion intermolecular structure influence the $CO_2$ coordination at higher concentrations of $CO_2$.

*$PF_6$ – $PF_6$ RDF.* Figure 2 presents the $PF_6$ – $PF_6$ RDF and the number integrals. The anion–anion radial distribution function varies significantly with increase in $CO_2$ concentration. Slight differences can be observed on addition of even 10 mol % of $CO_2$ to the ionic liquid. The differences also increase with $CO_2$ concentration. The position of the first peak in the g(r) shifts from 6.5 Å in the case of pure [bmim][$PF_6$] to a value of 8.1 Å at the highest concentration

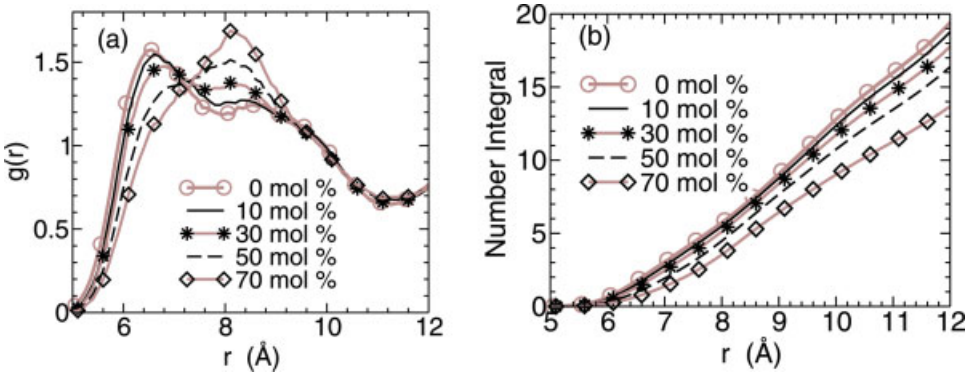


**Figure 2. (a) $PF_6$–$PF_6$ radial distribution functions at various $CO_2$ concentrations in the mixture; (b) corresponding number integrals.**

[Color figure can be viewed in the online issue, which is available at www.interscience.wiley.com.]

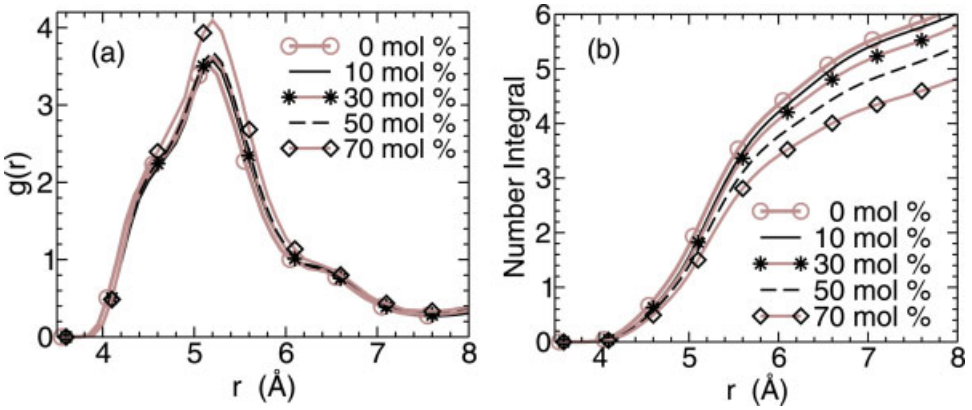


**Figure 3. (a) Radial distribution functions of $PF_6$ anions around the cation ring center at various concentrations of $CO_2$ in the mixture; (b) corresponding number integrals.**

[Color figure can be viewed in the online issue, which is available at www.interscience.wiley.com.]

of $CO_2$. The latter is comparable with the value of 7.95 Å, which was observed by Huang et al.[48] as the position of the first peak. The first peak broadens too with increasing concentration of $CO_2$. Anions move away from each other with increase in $CO_2$ concentration in the mixture. $CO_2$ molecules are preferentially located around the anions, and hence with an increase in their concentration, anions tend to be separated further. However, the position of the first minimum in the g(r) located at 11.2 Å is unaltered with increase in the $CO_2$ mole fraction.

As the anions move away from each other with introduction of $CO_2$, it is expected that the anion–anion coordination number will be lesser in case of mixture with highest concentration of $CO_2$ (see Figure 2b). The coordination numbers up to 7.2 Å (location where the intensity of all the RDF peaks is the same) are 3.3, 2.9, 2.3, and 1.7, respectively, for the 10, 30, 50, and 70 mol % mixtures. The same quantities up to the first minimum (at 11.2 Å) are 16.0, 15.2, 14.0, and 11.7, respectively.

*[bmim] – $PF_6$ RDF*. The cation–anion RDF is presented in Figure 3a, where the geometric center of the imidazolium ring is taken as the position of the cation. The corresponding number integrals are shown in Figure 3b. RDFs at all concentrations of $CO_2$ are similar. All of them peak at 5.6 Å with their first minima at 7.6 Å. The coordination numbers up to the first minimum are 5.7, 5.5, 5.1, and 4.6, respectively, for the 10, 30, 50, and 70 mol % mixtures of $CO_2$ – [bmim][$PF_6$]. The coordination number decreases with the increase in $CO_2$ concentration. This is similar to that seen in anion–anion RDF, where the specific interaction between anion and $CO_2$ was said to be the reason for the decrease in coordination number. However, it should be noted that the decrease in coordination number in the case of cation–anion is smaller when compared with that for the anion–anion. This suggests that the anion interaction with $CO_2$ is mainly responsible for the separation of ions.

The large changes observed in the behavior of anion–anion RDFs and the lack thereof in the anion–cation RDFs, as a function of $CO_2$ concentration provides evidence for the interaction between $CO_2$ and anion.

*$CO_2$–Ion RDF*. We shall now examine the $CO_2$–anion interaction from the perspective of $CO_2$. In Figure 4a, we show the RDF of $CO_2$–Phosphorus and that of $CO_2$–$C_r$ at two different concentrations of $CO_2$ in the mixture. $C_r$ is the

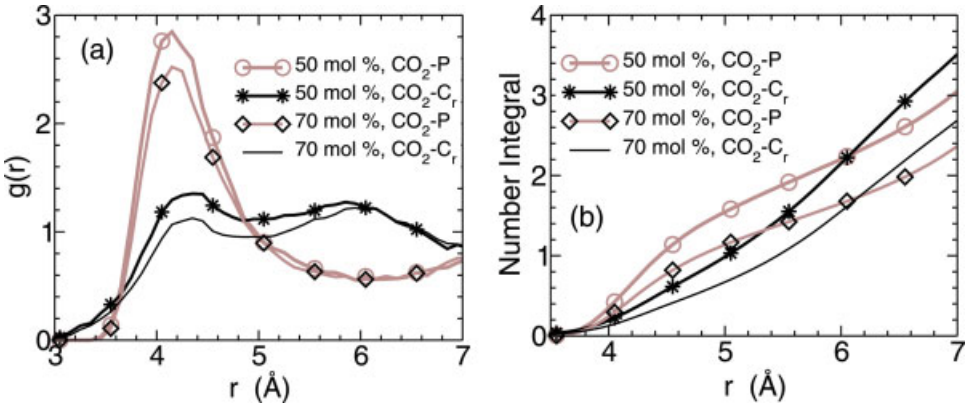


**Figure 4. (a) RDFs of $C(CO_2)$–P and $C(CO_2)$–$C_r$ at various concentrations of $CO_2$ in the solution and (b) corresponding number integrals.**

$C_r$ is the carbon atom present in between the two nitrogen atoms of the imidazolium (cation) ring. [Color figure can be viewed in the online issue, which is available at www.interscience.wiley.com.]

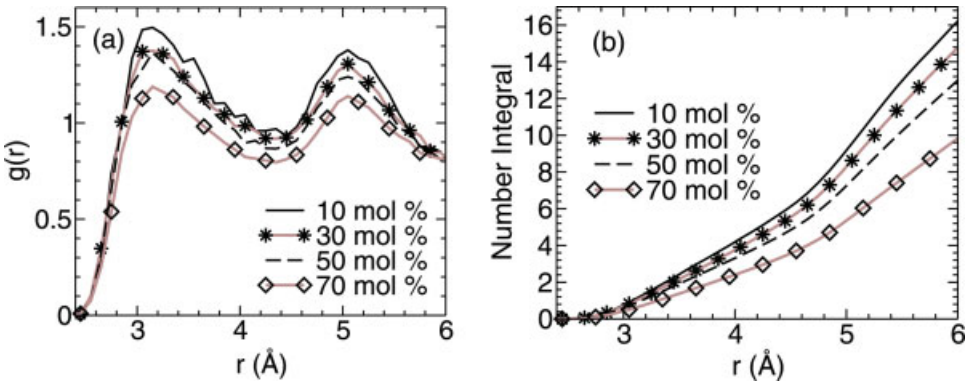


**Figure 5. (a) C($CO_2$)-fluorine radial distribution functions and (b) corresponding number integrals.**

[Color figure can be viewed in the online issue, which is available at www.interscience.wiley.com.]

ring carbon present in between the two ring nitrogens of the cation. Our ab initio MD simulations[53] had shown the presence of a weak hydrogen bond between the acidic hydrogen (which is covalently bonded to $C_r$) and the oxygen of $CO_2$. Hence, it is pertinent that we compare the $CO_2$–P RDF against the $CO_2$–$C_r$ one. From the magnitudes of the first peak, it is obvious that carbon dioxide has a larger preference for the anion than the cation (here, the $C_r$ site). This conclusion is confirmed from the number integrals shown in Figure 4b. In the 50 mol % mixture, at a distance of 5 Å, the number of anions surrounding a carbon dioxide is 1.6, whereas the number of cations ($C_r$ site) is only 1.0.

The specific nature of interaction between carbon dioxide and the anion is of Lewis acid–base type. In fact, this is true not only of the $PF_6$ anion studied here, but for a variety of $CO_2$–anion complexes.[60] The carbon atom of $CO_2$ (Lewis acid) interacts favorably with the lone pair on the fluorine of the anion (Lewis base). The C($CO_2$)-F RDF and the corresponding number integrals are shown in Figure 5 for all the mixtures studied. The strong peak in the RDFs present at 3.1 Å signifies specific interaction. At 10 mol % of $CO_2$, the number of fluorine atoms surrounding C($CO_2$) within a distance of 4.2 Å (the first minimum in the RDF) is around 5. This implies that the first coordination shell of a $CO_2$ molecule contains fluorine atoms from more than one $PF_6$ anion. Thus, $CO_2$ molecules mediate (and possibly diminish) ion–ion interactions.

### *Diffusion coefficients*

As an example, the mean squared displacement of anion and cation in the 30 mol % mixture that is obtained as an average over 5 independent configurations is presented in Figure 6, along with error bars. It can be seen from the figure that $CO_2$ molecules diffuse reasonably well. However, the ions have not diffused much within the time scale of the MSD plot. Experiments have shown a remarkable decrease in the viscosity of RTIL-$CO_2$ solution as a function of increasing $CO_2$ concentration.[38,45,61] Maginn and coworkers[62,63] as well as the group of Voth[18] have demonstrated the slow dynamics of ions in RTILs. If one plots the MSD vs. time data on a double log graph, the slope of the curve (denoted by $\beta$) should be unity for diffusive behavior. In the 30 mol % mixture, the values of $\beta$ at 500 ps were found to be 0.8, 0.7, and 0.98 for the cation, anion, and $CO_2$, respectively, whereas in the 70 mol % solution, the values were all above 0.95. Diffusion coefficients were calculated as the long-time regime slope of mean squared displacement curve (between 400 and 500 ps), for all concentrations of $CO_2$. In view of the fact that $\beta$ is slightly less than unity, the diffusion coefficient values should be construed as apparent estimates. The exact values are likely to be slightly higher.[62]

The diffusion coefficients of the ions as well as that of $CO_2$ molecules are found to increase with $CO_2$ concentration. It can be seen from the figure that the cation diffuses faster than the anion in [bmim][$PF_6$] – $CO_2$ mixtures which is also observed in experiments[64] as well as in simulations[30,54] of pure ionic liquids. The values of diffusion coefficients at various concentrations of $CO_2$ are presented in Table 3. In the pure IL, the apparent diffusion coefficients obtained from our model agrees within 20% of the experimental value.[54] Experimental data for diffusion coefficients in $CO_2$–[bmim][$PF_6$] solutions are not available. However, as mentioned earlier, the increased diffusivity of ions and of $CO_2$ in these solutions

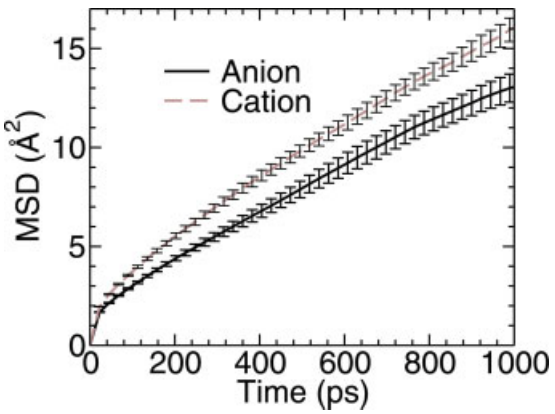


**Figure 6. Mean squared displacement of anion and cation at 300 K in the 30 mol % mixture of $CO_2$–[bmim][$PF_6$] obtained as an average over five independent blocks, shown along with error bars.**

[Color figure can be viewed in the online issue, which is available at www.interscience.wiley.com.]

**Table 3. Apparent Diffusion Coefficients of Anion, Cation, and $CO_2$ in the [bmim][$PF_6$] – $CO_2$ Mixture Obtained from Simulations at Different Concentration of $CO_2$**

| $CO_2$ (mol %) | $D_-$ ($\times 10^{-12}$ $m^2$ $s^{-1}$) | $D_+$ ($\times 10^{-12}$ $m^2$ $s^{-1}$) | $D_{CO_2}$ ($\times 10^{-12}$ $m^2$ $s^{-1}$) |
|---|---|---|---|
| 0 | 4.7 | 6.7 | – |
| 10 | 8.8 | 12.4 | 201.0 |
| 30 | 19.1 | 22.5 | 386.9 |
| 50 | 54.8 | 64.3 | 678.5 |
| 70 | 146.2 | 158.3 | 1453.8 |

The estimated uncertainty in the diffusion coefficient is 10%.

observed by us is consistent with the experimentally observed decrease in the viscosity of these solutions.[38,45,61]

The variation of diffusion coefficients with concentration of $CO_2$ along with the best fit for anions and cations is presented in Figure 7. The increase in diffusion of ions is slow at low $CO_2$ concentrations but becomes steeper as one proceeds toward higher concentration of $CO_2$. The diffusion coefficients were fitted to a cubic equation of the form,

$$D_{\pm} = a_0 + a_1 x + a_2 x^2 + a_3 x^3 \quad (1)$$

where $a_0$, $a_1$, $a_2$, $a_3$ are constants and $x$ is the mole fraction of $CO_2$ in the solution. The best fit values to curves that can be used to obtain diffusion coefficients values of ions and $CO_2$ at intermediate concentrations of $CO_2$ in the mixture are provided in Table 4. Huang et al[48] have carried out MD simulations of solutions of [bmim][$PF_6$] containing 76.6 mol % of $CO_2$. The diffusion coefficients of anion, cation, and $CO_2$ obtained using the cubic fit to our data at 76.6 mol % are 196, 210, and 1920 (all in units of $10^{-12}$ $m^2$ $s^{-1}$), respectively, whereas the values reported by Huang et al. are 68, 77, and 400 (all in units of $10^{-12}$ $m^2$ $s^{-1}$), respectively. In the absence of experimental values of diffusion coefficients in these mixtures, the differences could only be attributed to differences in the force fields.

### *Orientational relaxation*

The reorientational time correlation function for the OCO vector of $CO_2$ gives us an idea of the rotational relaxation

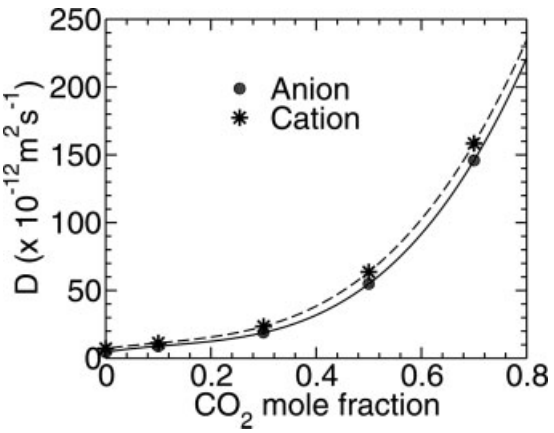


**Figure 7. Variation of diffusion coefficient of ions with concentration of $CO_2$ in the solution.**

The lines are cubic fits as expressed in Eq. 1.

**Table 4. Values from the Best Fit to Eq. 1 for Diffusion Coefficients of Anion, Cation and $CO_2$**

| Ion/Molecule | $a_0$ | $a_1$ | $a_2$ | $a_3$ |
|---|---|---|---|---|
| Anion | 4.6 | 59.5 | −221.3 | 606.8 |
| Cation | 7.2 | 50.8 | −155.5 | 559.6 |
| $CO_2$ | 2.4 | 2507.0 | −6582.7 | 8521.2 |

times involved. Figure 8 show this quantity in the solution at different concentrations of $CO_2$. It can be seen that the backbone vector of $CO_2$ decorrelates faster in the case of mixtures with higher concentration of $CO_2$. The correlation was found to be lost completely before 120 ps in all the systems studied. These correlation functions show biexponential decay with two different relaxation times, one of the order of picoseconds and the other, in tens of picoseconds. The amplitude and the relaxation times obtained by fitting the data (up to 120 ps) to a constrained biexponential function of the form

$$y = a\ \exp(-t/\tau_1) + (1-a)\ \exp(-t/\tau_2) \quad (2)$$

are tabulated in Table 5.

The faster relaxation for the systems with higher concentration of $CO_2$ can be observed at both timescales. The total relaxation is almost equally divided between these two time scales, which is evident from the amplitudes that are close to 0.5. The variation of the relaxation times with the $CO_2$ concentration shows a near linear behavior for both the timescales and also their amplitude weighted average. In summary, the $CO_2$ rotation is less hindered in the [bmim][$PF_6$] – $CO_2$ mixtures with higher mole fraction of $CO_2$, due possibly to reduced ion–ion interactions.

## Conclusions

Molecular dynamics simulation studies have been carried out on [bmim][$PF_6$] – $CO_2$ mixtures at varying concentrations of $CO_2$. The expansion in the volume of the solutions

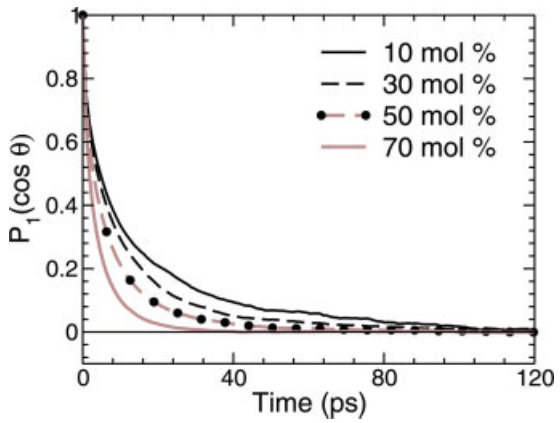


**Figure 8. Reorientational time correlation function of the OCO vector of $CO_2$ at various concentrations of $CO_2$ in the solution.**

[Color figure can be viewed in the online issue, which is available at www.interscience.wiley.com.]

**Table 5. Amplitude of Relaxation and the Relaxation Times for the Reorientation of OCO Vector for Different Mole Fractions of $CO_2$ in [bmim][$PF_6$] – $CO_2$ Mixture**

| $CO_2$ (mole %) | $a$ | $\tau_1$ (ps) | $\tau_2$ (ps) |
|---|---|---|---|
| 10 | 0.539 | 2.560 | 26.53 |
| 30 | 0.474 | 1.882 | 16.96 |
| 50 | 0.479 | 1.574 | 11.57 |
| 70 | 0.463 | 1.035 | 6.140 |

The statistical uncertainty in the time constants is 10%.

determined from simulations agree well with experimental data. Trends in the radial distribution of anions around an anion as well as that of anions around the cation indirectly suggest specific anion–$CO_2$ interaction. The nature of such an interaction (Lewis acid–base type) has been documented by us earlier.[53,60] This aspect is also seen in the anion–$CO_2$ radial distribution function. The diffusion coefficient of the ions and of $CO_2$ increases with increase in $CO_2$ concentration. This nonlinear increase has been fitted to a cubic equation, which can be used to obtain the diffusion coefficients at intermediate values of $CO_2$ concentrations that have not been studied. The reorientational relaxation of the $CO_2$ molecule is found to be biexponential in time. The mean relaxation time decreases with increasing concentration of $CO_2$.

It is hoped that molecular simulations would considerably help in a microscopic understanding of gas solubilities in ionic liquids.[65]

## Acknowledgments

The research reported here is supported by the Department of Science and Technology, Government of India. B.L.B. thanks CSIR, India, for a research fellowship.

## Literature Cited

1. Brennecke JF, Maginn EJ. Ionic liquids: innovative fluids for chemical processing. *AIChE J*. 2001;47:2384–2389.
2. Clarke MJ, Harrison KL, Johnston KP, Howdle SM. Water in supercritical carbon dioxide microemulsions: spectroscopic investigation of a new environment for aqueous inorganic chemistry. *J Am Chem Soc*. 1997;119:6399.
3. Nagashima K, Lee CT Jr, Xu B, Johnston KP, DeSimone JM, Johnson CS Jr. NMR studies of water transport and proton exchange in water-in-carbon dioxide microemulsions. *J. Phys. Chem B*. 2003; 107:1962–1968.
4. Chen B, Siepmann JI, Klein ML. Direct Gibbs ensemble Monte Carlo simulations for solid-vapor phase equilibria: applications to Lennard-Jonesium and carbon dioxide. *J Phys Chem B*. 2001;105: 9840–9848.
5. Salaniwal S, Cui ST, Cummings PT, Cochran HD. Self-assembly of reverse micelles in water/surfactant/carbon dioxide systems by molecular simulation. *Langmuir* 1999;15:5188.
6. Salaniwal S, Cui ST, Cochran HD, Cummings PT. Molecular simulation of a dichain surfactant water carbon dioxide system. I. Structural properties of aggregates. *Langmuir*. 2001;17:1773–1783.
7. Senapati S, Keiper JS, DeSimone JM, Wignall GD, Melnichenko YB, Frielinghaus H, Berkowitz ML. Structure of phosphate fluorosurfactant based reverse micelles in supercritical carbon dioxide. *Langmuir*. 2002;18:7371–7376.
8. Wasserscheid P. Volatile times for ionic liquids. *Nature* 2006;439: 797
9. Earle MJ, Esperanca JMSS, Gilea MA, Lopes JNC, Rebelo LPN, Magee JW, Seddon KR, Widegren JA. The distillation and volatility of ionic liquids. *Nature*. 2006;439:831–834.
10. Welton T. Room-temperature ionic liquids. Solvents for synthesis and catalysis. *Chem Rev*. 1999;99:2071–2083.
11. Earle MJ, Seddon KR. Ionic liquids. Green solvents for the future. *Pure Appl Chem*. 2000;72:1391–1398.
12. Triolo A, Mandanici A, Russina O, Rodriguez-Mora V, Cutroni M, Hardacre C, Nieuwenhuyzen M, Bleif H, Keller L, Ramos MA. Thermodynamics, structure, and dynamics in room temperature ionic liquids: the case of 1-butyl-3-methyl imidazolium hexafluorophosphate ([bmim][$PF_6$]). *J Phys Chem B*. 2006;110:21357–21364.
13. Berg RW, Deetlefs M, Seddon KR, Shim I, Thompson JM. Raman and ab initio studies of simple and binary 1-alkyl-3-methylimidazolium ionic liquids. *J Phys Chem B*. 2005;109:19018–19025.
14. Hanke CG, Price SL, Lynden-Bell RM. Intermolecular potentials for simulations of liquid imidazolium salts. *Mol Phys*. 2001;99:801–809.
15. Hanke CG, Atamas NA, Lynden-Bell RM. Solvation of small molecules in imidazolium ionic liquids: a simulation study. *Green Chem*. 2002;4:107–111.
16. Lynden-Bell RM, Atamas NM, Vasilyuk A, Hanke CG. Chemical potentials of water and organic solutes in imidazolium ionic liquids: a simulation study. *Mol Phys*. 2002;100:3225–3229.
17. Lynden-Bell RM. Gas-liquid interfaces of room temperature ionic liquids. *Mol Phys*. 2003;101:2625–2633.
18. Del-Popolo MG, Voth GA. On the structure and dynamics of ionic liquids. *J Phys Chem B*. 2004;108:1744–1752.
19. Lynden-Bell RM, Kohanoff J, Del Popolo MG. Simulation of interfaces between room temperature ionic liquids and other liquids. *Faraday Discuss*. 2005;129:57–67.
20. Hu Z, Margulis CJ. Heterogeneity in a room-temperature ionic liquid: persistent local environments and red-edge effect. *Proc Natl Acad Sci USA*. 2006;103:831–836.
21. Yan T, Li S, Jiang W, Gao X, Xiang B, Voth GA. Structure of the liquid-vacuum interface of room-temperature ionic liquids: a molecular dynamics study. *J Phys Chem B*. 2006;110:1800.
22. Karmakar R, Samanta A. Dynamics of solvation of the fluorescent state of some electron donor-acceptor molecules in room temperature ionic liquids, [BMIM][$(CF_3SO_2)_2$N] and [EMIM][$(CF_3SO_2)_2$N]. *J Phys Chem A*. 2003;107:7340–7346.
23. Yan T, Burnham CJ, Del Popolo MG, Voth GA. Molecular dynamics simulation of ionic liquids: the effect of electronic polarizability. *J Phys Chem B*. 2004;108:11877–11881.
24. Wang Y, Voth GA. Unique spatial heterogeneity in ionic liquids. *J Am Chem Soc*. 2005;127:12192–12193.
25. Tsuzuki S, Tokuda S, Hayamizu K, Watanabe M. Magnitude and directionality of interaction in ion pairs of ionic liquids: relationship with ionic conductivity. *J Phys Chem B*. 2005;109:16474–16481.
26. Hunt PA. The simulation of imidazolium-based ionic liquids. *Mol Sim*. 2006;32:1–10.
27. Kobmann S, Thar J, Kirchner B, Hunt PA, Welton T. Cooperativity in ionic liquids. *J Chem Phys*. 2006;124:174506.
28. Hunt PA, Kirchner B, Welton T. Characterising the electronic structure of ionic liquids: an examination of the 1-butyl-3-methylimidazolium chloride ion pair. *Chem Eur J*. 2006;12:6762–6775.
29. Hunt PA, Gould IR. Structural characterization of the 1-butyl-3-methylimidazolium chloride ion pair using a initio methods. *J Phys Chem A*. 2006;110:2269–2282.
30. Bhargava BL, Balasubramanian S. Dynamics in a room temperature ionic liquid: a computer simulation study of 1,3-dimethylimidazolium chloride. *J Chem Phys*. 2005;123:144505; *ibid Erratum*. 2006;125:219901.
31. Gong L, Guo W, Xiong J, Li R, Wu X, Li W. Structures and stability of ionic liquid model with imidazole and hydrogen fluorides chains: density functional theory study. *Chem Phys Lett*. 2006;425: 167–178.
32. Wang Y, Li H, Han S. The chemical nature of the C-H. . .$X^-$ (X = Cl or Br) interaction in imidazolium halide ionic liquids. *J Chem Phys*. 2006;124:044504.
33. Blanchard LA, Hancu D, Beckman EJ, Brennecke JF. Green processing using ionic liquids and $CO_2$. *Nature*. 1999;399:28–29.
34. Cole-Hamilton DJ. Homogeneous catalysis—new approaches to catalyst separation, recovery, and recycling. *Science*. 2003;299:1702–1706.
35. Scurto AM, Aki SNVK, Brennecke JF. $CO_2$ as a separation switch for ionic liquid/organic mixtures. *J Am Chem Soc*. 2002;124:10276–10277.
36. Scurto AM, Leitner W. Expanding the useful range of ionic liquids: melting point depression of organic salts with carbon dioxide for biphasic catalytic reactions. *Chem Commun*. 2006;3681–3683.

37. Fletcher KA, Baker SN, Baker GA, Pandey S. Probing solute and solvent interactions within binary ionic liquid mixtures. *New J Chem*. 2003;27:1706–1712.
38. Blanchard LA, Gu Z, Brennecke JF. High-pressure phase behavior of ionic liquid/$CO_2$ systems. *J Phys Chem B*. 2001;105:2437–2444.
39. Anthony JL, Maginn EJ, Brennecke JF. Solubilities and thermodynamic properties of gases in the ionic liquid 1-*n*-butyl-3-methylimidazolium hexafluorophosphate. *J Phys Chem B*. 2002;106:7315–7320.
40. Kamps AP, Tuma D, Xia J, Maurer G. Solubility of $CO_2$ in the ionic liquid [bmim][$PF_6$]. *J Chem Eng Data*. 2003;48:746–749.
41. Husson-Borg P, Majer V, CostaGomes MF. Solubilities of oxygen and carbon dioxide in butyl methyl imidazolium tetrafluoroborate as a function of temperature and at pressures close to atmospheric pressure. *J Chem Eng Data*. 2003;48:480–485.
42. Anthony JL, Anderson JL, Maginn EJ, Brennecke JF. Anion effects on gas solubility in ionic liquids. *J Phys Chem B*. 2005;109:6366–6374.
43. Muldoon MJ, Aki SNVK, Anderson JL, Dixon JK, Brennecke JF. Improving carbon dioxide solubility in ionic liquids. *J Phys Chem B*. 2007;111:9001–9009.
44. Kazarian SG, Briscoe BJ, Welton T. Combining ionic liquids and supercritical fluids: in situ ATR-IR study of $CO_2$ dissolved in two ionic liquids at high pressures. *Chem Commun*. 2000;2047–2048.
45. Lu J, Liotta CL, Eckert CA. Spectroscopically probing microscopic solvent properties of room-temperature ionic liquids with the addition of carbon dioxide. *J Phys Chem A*. 2003;107:3995–4000.
46. Cadena C, Anthony JL, Shah JK, Morrow TI, Brennecke JF, Maginn EJ. Why is $CO_2$ so soluble in imidazolium-based ionic liquids? *J Am Chem Soc*. 2004;126:5300–5308.
47. Deschamps J, Costa Gomes MF, Pádua AAH. Molecular simulation study of interactions of carbon dioxide and water with ionic liquids. *ChemPhysChem*. 2004;5:1049–1052.
48. Huang X, Margulis CJ, Li Y, Berne BJ. Why is the partial molar volume of $CO_2$ so small when dissolved in a room temperature ionic liquid? Structure and dynamics of $CO_2$ dissolved in [$bmim^+$][$PF_6^-$]. *J Am Chem Soc*. 2005;127:17842–17851.
49. Kanakubo M, Umecky T, Hiejima Y, Aizawa T, Nanjo H, Kameda Y. Solution structures of 1-butyl-3-methylimidazolium hexafluorophosphate ionic liquid saturated with CO2: experimental evidence of specific anion-$CO_2$ interaction. *J Phys Chem B*. 2005;109:13847–13850.
50. Kroon MC, Karakatsani EK, Economou IG, Witkamp G, Peters CJ. Modeling of the carbon dioxide solubility in imidazolium-based ionic liquids with the tPC-PSAFT equation of state. *J Phys Chem B*. 2006;110:9262–9269.
51. Yu G, Zhang S, Zhou G, Liu X, Chen X. Structure, interaction and property of amino-functionalized imidazolium ILs by molecular dynamics simulation and ab initio calculation. *AIChE J*. 2007;53:3210–3221.
52. Fredlake CP, Muldoon MJ, Aki SNVK, Welton T, Brennecke JF. Solvent strength of ionic liquid/$CO_2$ mixtures. *Phys Chem Chem Phys*. 2004;6:3280–3285.
53. Bhargava BL, Balasubramanian S. Insights into the structure and dynamics of a room temperature ionic liquid: ab initio molecular dynamics simulation studies of [bmim][$PF_6$] and the [bmim][$PF_6$] – $CO_2$ mixture. *J Phys Chem B*. 2007;111:4477–4487.
54. Bhargava BL, Balasubramanian S. A refined potential model for atomistic simulations of an ionic liquid, [bmim][$PF_6$]. *J Chem Phys*. 2007;127:114510.
55. Tuckerman ME, Yarne DA, Samuelson SO, Hughes AL, Martyna GJ. Exploiting multiple levels of parallelism in molecular dynamics based calculations via modern techniques and software paradigms on distributed memory computers. *Comput Phys Commun*. 2000;128:333–376.
56. Borodin O, Smith GD, Jaffe RL. Ab initio quantum chemistry and molecular dynamics simulations studies of $LiPF_6$/poly(ethylene oxide) interactions. *J Comput Chem*. 2001;22:641–654.
57. Aki SNVK, Mellein BR, Saurer EM, Brennecke JF. High-pressure phase behavior of carbon dioxide with imidazolium-based ionic liquids. *J Phys Chem B*. 2004;108:20355–20365.
58. Martyna GJ, Klein ML, Tuckerman ME. Nosé-Hoover chains: the canonical ensemble via continuous dynamics. *J Chem Phys*. 1992;97:2635–2643.
59. Tuckerman ME, Berne BJ, Martyna GJ. Reversible multiple time scale molecular dynamics. *J Chem Phys*. 1992;97:1990–2001.
60. Bhargava BL, Balasubramanian S. Probing anion-carbon dioxide interactions in room temperature ionic liquids: gas phase cluster calculations. *Chem Phys Lett*. 2007;444:242–246.
61. Tomida D, Kumagai A, Qiao K, Yokoyama C. Viscosity of 1-butyl-3-methylimidazolium hexafluorophosphate + $CO_2$ mixture. *J Chem Eng Data*. 2007;52:1638–1640.
62. Cadena C, Zhao Q, Snurr RQ, Maginn EJ. Molecular modeling and experimental studies of the thermodynamic and transport properties of pyridinium-based ionic liquids. *J Phys Chem B*. 2006;110:2821–2832.
63. Maginn EJ. Atomistic simulation of the thermodynamic and transport properties of ionic liquids. *Acc Chem Res*. 2007;40:1200–1207.
64. Tokuda H, Hayamizu K, Ishii K, Susan MABH, Watanabe M. Physicochemical properties and structures of room temperature ionic liquids. I. Variation of anionic species. *J Phys Chem B*. 2004;108:16593–16600.
65. Anderson JL, Dixon JK, Brennecke JF. Solubility of $CO_2$, $CH_4$, $C_2H_6$, $C_2H_4$, $O_2$, and $N_2$ in 1-hexyl-3-methylpyridinium bis(trifluoromethylsulfonyl)imide: comparison to other ionic liquids. *Acc Chem Res*. 2007;40:1208–1216.

*Manuscript received Jan. 28, 2008, revision received Apr. 21, 2008, and final revision received Jun. 20, 2008.*